

INFLUENCE OF HELIUM ION IMPLANTATION ON OPTICAL PROPERTIES OF FUSED SILICA

M. Zhong¹, J. H. Li¹, B. Li², C. X. Tian², X. Xiang², C. Zhou³, W. F. Yang^{1*}

¹ Aviation Engineering Institute at Civil Aviation Flight University of China, Guanghan 618307, China; e-mail: ywfcyy@163.com

² School of Physics at University of Electronic Science and Technology of China, Chengdu 610054, China

³ Key Laboratory of Flight Techniques and Flight Safety, CAAC, Civil Aviation Flight University of China, Guanghan 618307, China

High-purity fused silica has been implanted with 60-keV helium ions at the fluence of $1.5 \cdot 10^{17} \text{ cm}^{-2}$. The effects of helium-ion implantation on optical properties of silica samples before and after helium implantation have been investigated by infrared (IR), photoluminescence (PL), and ultraviolet-visible (UV-vis) spectrophotometer. After helium-ion implantation, X-ray photoelectron spectroscopy (XPS) results indicate that Si 2p peak is shifted to higher binding energy. An obvious PL band at 500 nm is observed, and the PL intensity is significantly decreased. However, the intensity of IR and optical absorption is increased greatly by ion implantation. A mechanism for the effects of helium implantation on optical properties of fused silica is discussed.

Keywords: helium-ion implantation, fused silica, photoluminescence, X-ray photoelectron spectroscopy, infrared, ultraviolet-visible spectrophotometer.

ВЛИЯНИЕ ИОННОЙ ИМПЛАНТАЦИИ ГЕЛИЯ НА ОПТИЧЕСКИЕ СВОЙСТВА ПЛАВЛЕНОГО КВАРЦА

M. Zhong¹, J. H. Li¹, B. Li², C. X. Tian², X. Xiang², C. Zhou³, W. F. Yang^{1*}

УДК 535.37:535.561

¹ Авиационный инженерный институт Университета гражданской авиации Китая, Гуанхань 618307, Китай; e-mail: ywfcyy@163.com

² Школа физики Китайского университета электронных наук и технологий, Чэнду 610054, Китай

³ Университет гражданской авиации Китая, Гуанхань 618307, Китай

(Поступила 12 марта 2020)

Высокоочищенный плавленый кварц имплантирован ионами гелия с энергией 60 кэВ потоком $1.5 \times 10^{17} \text{ см}^{-2}$. Исследовано влияние имплантации ионов гелия на оптические свойства образцов кремния до и после имплантации гелия с помощью инфракрасной, фотолюминесцентной и УФ-видимой спектрофотометрии. После имплантации ионов гелия результаты рентгеновской фотоэлектронной спектроскопии показывают, что пик Si 2p смещен в сторону более высокой энергии. Наблюдается полоса фотолюминесценции (ФЛ) на 500 нм, при этом интенсивность ФЛ значительно снижается. Однако интенсивности ИК-излучения и оптического поглощения значительно увеличиваются при имплантации ионов. Обсуждается механизм влияния имплантации гелия на оптические свойства плавленого кварца.

Ключевые слова: гелий-ионная имплантация, плавленый кварц, фотолюминесценция, рентгеновская фотоэлектронная спектроскопия, инфракрасный, ультрафиолетовый и видимый спектрофотометр.

Introduction. Fused silica, amorphous SiO₂, has attracted increasing interest due to its excellent properties and wide application, especially, in meeting the urgent demands of engineering [1]. In fact, silica has been used extensively been used as electronic and optical components in future fusion devices, in which helium is produced by (n, α) reactions [2]. Ion implantation can not only simulate the condition of fusion reactions, but

also can improve the investigate of the generation mechanisms and evolution of defects induced by irradiation in the near-surface region of silica. Furthermore, ion implantation has been found to be a very effective technique for surface modification [3, 4]. After low-energy-ion implantation, most of the ion energy is deposited at the surface of silica, resulting in ionization, atomic displacement, and sputtering [5]. Consequently, helium irradiation/implantation, resulting from the reaction and/or ion implantation, will inevitably affect the properties of silica, including optical, electronic and magnetic properties. It is known that the irradiation/implantation can induce optical absorption and luminescence bands in silica [6, 7]. All of these optical effects are caused, or at least initiated, by the production of point defects, which is mainly attributed to nuclear collisions.

Previously, researchers have studied microstructure, electrical, and physical properties of silica implanted with ions, such as surface electrical degradation, defect formation [8], optical absorption [9, 10], and luminescence [11–13]. However, the effect of helium ions implantation on the optical properties of fused silica and its mechanisms remains to be necessary for further investigation. Based on this motivation, in this work, 60 keV helium-ion implanted fused silica at the fluence of $1.5 \cdot 10^{17} \text{ cm}^{-2}$ at room temperature was first investigated, then the helium-ion-beam induced optical absorption and photoluminescence (PL) was analyzed, and an attempt was made to explain the damage process mechanism.

Experimental details. High-purity silica with two-sided optically polished surfaces was used. The size of the silica sample was $10 \times 10 \times 0.5 \text{ mm}$. The laminar sample, provided by a commercial company, was implanted with 60-keV helium ions at the fluence of $1.5 \cdot 10^{17} \text{ cm}^{-2}$ using a multifunctional ion implanter at room temperature. During the process of ion implantation, the vacuum was controlled at $2.0 \cdot 10^{-3} \text{ Pa}$, and the ion-beam current density was $17 \mu\text{A}/\text{cm}^2$. The stopping and range of ions in matter (SRIM) program was used to calculate the distribution of He impurities and the damage level caused by ions [14], SRIM can calculate many features of the transport of ions in matter. X-ray photoelectron spectroscopy (XPS) measurements were conducted using a Kratos XSAM 800 to observe the chemical composition and valence state of the samples. The optical-absorption spectra were measured by a SHIMADZU UV-2550 ultraviolet-visible spectrophotometer. PL spectra were obtained by a Perkin-Elmer LS55 fluorescence spectrophotometer. A Nicolet 950 attenuated total reflection Fourier-transform infrared (FT-IR) spectrometer within the range $650\text{--}4000 \text{ cm}^{-1}$ was used to acquire the IR spectra at room temperature.

Results and discussion. To understand the collision process between the incident ions and target material, and to achieve the accuracy and controllability of the ion-implantation process [15], SRIM was used to simulate and calculate the implanted helium atomic concentration and displacement per atom (dpa), which can effectively be used to determine the distribution and depth of ion implantation as well as the ion-induced damage level. For calculation, the silica density was $2.27 \text{ g}/\text{cm}^3$, and a displacement energy value of SiO_2 was $E_d = 20 \text{ eV}$ [16]. The SRIM calculation result of 60 keV, $1.5 \cdot 10^{17}/\text{cm}^2$ helium-ion implanted silica is shown in Fig. 1, which has clearly show that the distribution of helium impurities and the profile of the helium-ion-induced damage level are both exhibit a Gaussian distribution. The maximum penetration depth is approximately 750 nm and the maximum helium ions concentration is $4.5 \cdot 10^{21} \text{ cm}^{-3}$ at a depth of 560 nm. In addition, in the case of helium ions implantation, there are ionization and atomic displacement occur in the near-surface region, which can produce approximately 8.2 DPA at a depth of 480 nm.

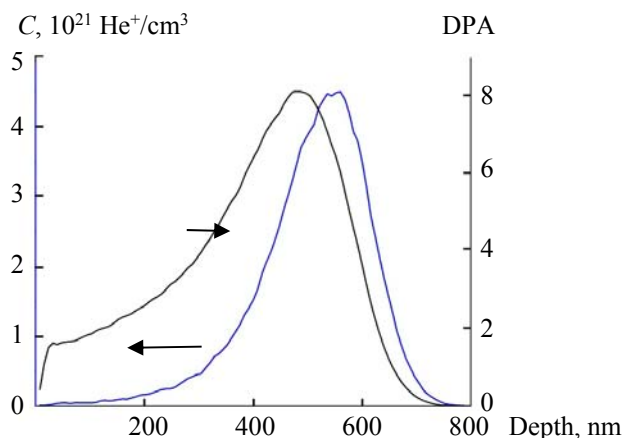


Fig. 1. SRIM calculations of 60 keV, $1.5 \cdot 10^{17}/\text{cm}^2$ helium-ion implanted fused silica.

XPS analysis. To analyze the elemental chemical state of silica samples before and after helium ions implantation, the O 1s and Si 2p photoelectron peaks were obtained from the measured spectra to determine elemental concentrations consistent with the nominal sample composition. XPS analysis of helium-ion implanted fused silica is demonstrated in Fig. 2. It is clearly shown that a photoelectron peak at approximately 532 eV appears, as shown in Fig. 2a, representing the electronic state of O 1s. Additionally, it is evidence that Si 2p peak, at approximately 103 eV, is shifted to higher binding energy, as shown in Fig. 2b, which occurs approximately 1 eV. It is probably because that the electron charge density around Si atom is decreased, a transfer of electronic charge to the neighbouring oxygen is occurred after helium ions implantation [17].

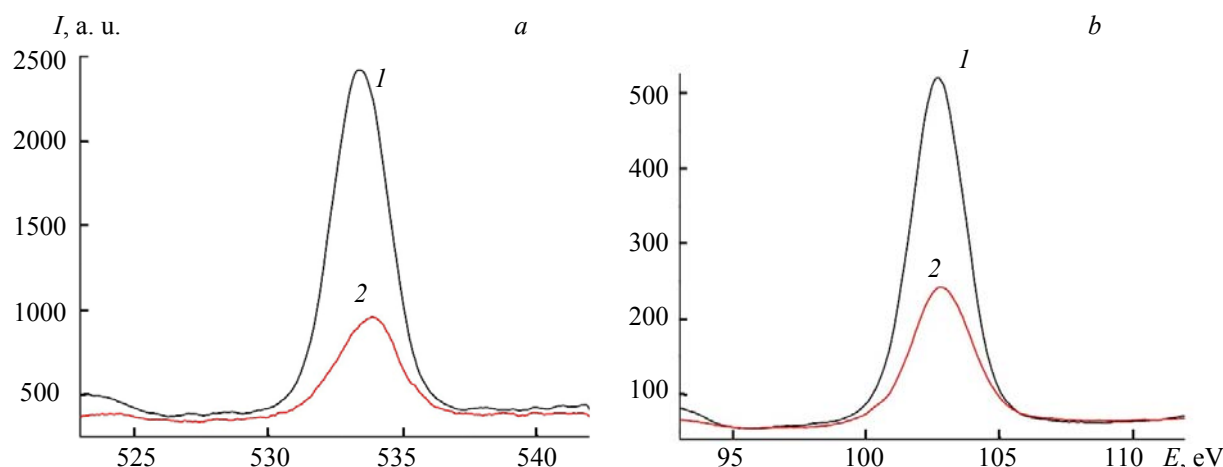


Fig. 2. XPS analysis of helium-ion implanted fused silica:
1 — SiO₂, 2 — He · SiO₂, (a) O 1s, (b) Si 2p.

IR spectrum analysis. To explore the ion-beam-induced changes of surface molecular structures, the IR absorption spectra of fused silica samples are analyzed for comparison before and after helium ions implantation. The IR spectra of helium-implanted fused silica are shown in Fig. 3. It is found that IR absorption intensity of silica increases significantly after helium ions implantation. The two spectra both have three obvious absorption peaks in the ranges of 750–900, 900–1100, and 1100–1300 cm⁻¹, which are centered at approximately 800, 1045, and 1150 cm⁻¹, respectively. It has been reported that these three peaks are mainly attributed to the bending, transverse-optical, and longitudinal optical vibrations of the asymmetric tensile vibration Si-O-Si, respectively [18]. In addition, there is a shift from 1150 to 1120 cm⁻¹ in the IR absorption spectra, and the IR shift of peak positions shows that the surface molecular structures have been significantly changed after helium ions implantation.

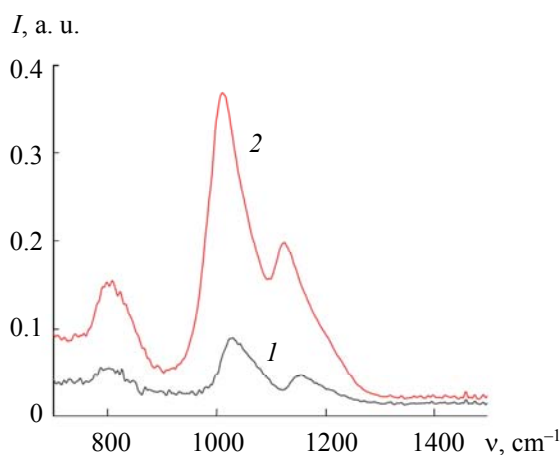


Fig. 3. IR spectra of helium-ion implanted fused silica, 1 — SiO₂, 2 — He · SiO₂.

Absorption spectrum analysis. The optical absorption spectra of helium-ion implanted fused silica are shown in Fig. 4. It is obviously shown that optical absorption intensity of silica increases greatly after helium ions implantation. Obviously, the optical absorption centers, attributed to point defects, are produced by helium ions implantation, and the formation of optical absorption centers is involved in the increasing intensity of silica. Based on the previous study [7], it is reasonable to conclude that optical absorption is related to the defects, which can be produced by the displacement of glass network atoms, or by the population of pre-existing or by ionization charges. However, the samples having low-OH content used in the present work are high purity, with the pre-existing defects produced by manufacturing.

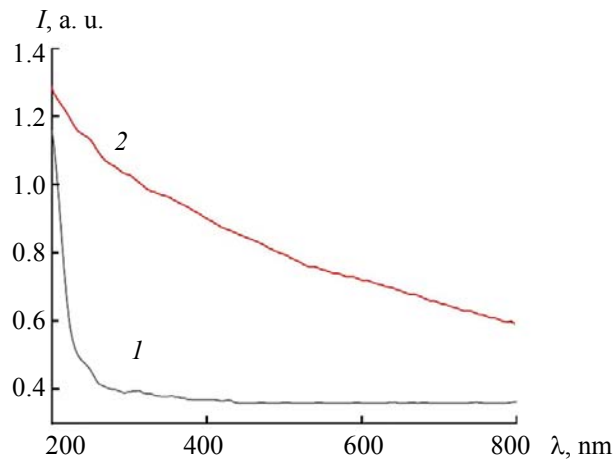


Fig. 4. Optical absorption spectra of helium-ion implanted fused silica, 1 — SiO_2 , 2 — $\text{He} \cdot \text{SiO}_2$.

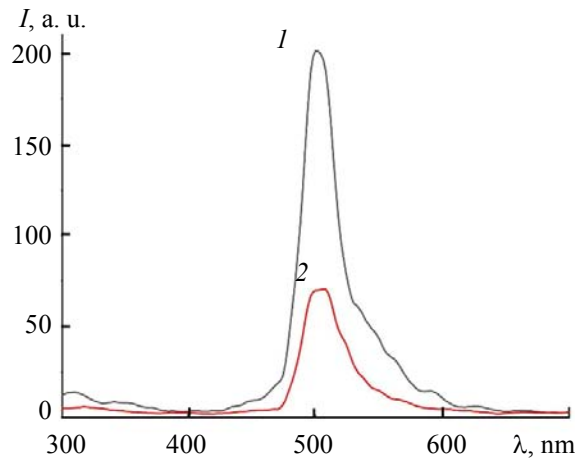


Fig. 5. PL spectra of helium-ion implanted fused silica, 1 — SiO_2 , 2 — $\text{He} \cdot \text{SiO}_2$.

PL spectrum analysis. To understand the dynamic process of defect formation, the ion-induced luminescence of silica was investigated. The PL spectra of helium-ion implanted fused silica are shown in Fig. 5. It is clearly shown that a narrow PL band at 500 nm (2.48 eV), ascribed to an E' -center, is observed. Oxygen-deficiency-related defects (E' -center) were produced by atomic displacement during helium ions implantation. Therefore, ion-induced luminescence was caused by an oxygen vacancy assisted by electron excitation. Obviously, the PL band intensity at 500 nm decreases significantly after helium ions implantation, which is related to the annihilation of defects. After ion implantation, the electron energy was deposited on the surface of fused silica, resulting in the reduction of defect concentration. Therefore, defect-concentration evolution has a great influence on the properties of ion-induced luminescence.

Conclusions. The effect of helium ions implantation on the optical properties of fused silica is highly significant. After helium ions implantation, Si 2p peak shifts to higher binding energy probably due to a transfer of electronic charge, and the intensity of IR and optical absorption increases greatly by ion implantation. The optical absorption centers are related to the defects, which can be produced by the displacement of glass network atoms, or by ionization charges. The PL band intensity at 500 nm decreases significantly, which is probably attributed to the annihilation of defects. The primary mechanism for the change of optical properties is the formation and annihilation of optical active defects in fused silica by ion implantation.

Acknowledgments. This work was supported by the National Natural Science Foundation of China (Grant No. U1830204), National Key R&D Program of China (Grant No. 2018YFC0809500), Key Project of Sichuan Department of Science and Technology (Grant No. 2018GZ0497), and project of Civil Aviation Flight University of China (Grant Nos. BJ2016-04, J2018-56, and CJ2019-01). The authors would like to thank Let Pub for its linguistic assistance during the preparation of this manuscript.

REFERENCES

1. M. Zhong, G. X. Yang, Z. H. Yan, L. Yang, *Optik*, **127**, No. 8, 3853–3857 (2016).
2. A. Ibarra, E. R. Hodgson, *Nucl. Instr. Method. B*, **218**, 29–35 (2004).
3. X. Xiang, X. T. Zu, S. Zhu, *Appl. Phys. Lett.*, **84**, No. 1, 52–54 (2004).
4. M. Zhong, L. Yang, H. H. Shen, *Nucl. Instrum. Methods B*, **353**, 21–27 (2015).
5. S. M. Gonzalez de Vicente, A. Morono, E. R. Hodgson, *Fusion Eng. Des.*, **84**, No. 2-6, 837–839 (2009).
6. S. Nagata, H. Katsui, B. Tsuchiya, *J. Nucl. Mater.*, **386-388**, 1045–1048 (2009).
7. M. L. Crespillo, J. T. Graham, Y. Zhang, *J. Lumin.*, **172**, 208–218 (2016).
8. S. Nagata, S. Yamamoto, A. Inouye, *J. Nucl. Mater.*, **367-370**, 1009–1013 (2007).
9. P. Martin, D. Jimenez-Rey, R. Vila, *Fusion Eng. Des.*, **89**, No. 7-8, 1679–1683 (2014).
10. Y. J. Chu, G. F. Wang, L. Zheng, *Surf. Coat. Technol.*, **348**, 91–96 (2018).
11. V. Zhurenko, O. Kalantaryan, S. Kononenko, *Nucl. Instrum. Method. B*, **407**, 5–9 (2017).
12. D. Bachiller-Perea, D. Jimenez-Rey, A. Munoz-Martin, *J. Non-Cryst. Solids*, **428**, 36–41 (2015).
13. K. Furumoto, T. Tanabe, *J. Nucl. Mater.*, **442**, No. 1-3, S511–S514 (2013).
14. J. F. Ziegler, M. D. Ziegler, J. P. Biersack, *Nucl. Instrum. Methods B*, **268**, No. 11-12, 1818–1823 (2010).
15. W. Q. Li, X. Y. Zhan, X. Y. Song, *Small*, **23**, No. 31, 1901820 (2019).
16. H. Amekura, O. A. Plaksin, N. Kishimoto, *Jpn. J. Appl. Phys.*, **40**, No. 2B, 1091–1093 (2001).
17. V. Simon, M. Todea, A. F. Takacs, *Solid State Commun.*, **141**, No. 1, 42–47 (2007).
18. B. Li, X. Xiang, W. Liao, *Appl. Surf. Sci.*, **471**, 786–794 (2019).